

RELATIVE INTENSITIES IN X-RAY PHOTOELECTRON SPECTRA

Part VII The effect of elastic scattering in a solid on the angular distribution of photoelectrons escaping from samples covered with thin films of various thicknesses*

O A BASCHENKO and V I NEFEDOV

*Institute of General and Inorganic Chemistry, Academy of Sciences of the U S S R ,
Moscow (U S S R)*

(Received 19 May 1980)

ABSTRACT

The angular distributions of X-ray photoelectron peak intensity for (1) a semi-infinite sample, (2) a substrate sample covered with a film, and (3) an overlayer sample are calculated by the Monte-Carlo method. The elastic as well as the inelastic scattering of electrons in a solid is taken into account. In all cases the elastic scattering is shown to have a significant effect on both the absolute value of peak intensity and the angular distribution of photoelectrons. The electron mean free paths without inelastic collisions (λ_n) calculated using formulas derived without taking account of elastic scattering are shown to differ significantly from the real values. Moreover, the λ_n values calculated in this way are not physical constants at all, but depend for example on the film thickness and the intervals of photoelectron take-off angles under consideration. The elastic scattering effect is shown capable of explaining some difficulties which arise in the interpretation of experimental data reported in the literature on the basis of expressions derived taking into account only the inelastic interactions of photoelectrons with a solid.

INTRODUCTION

In an earlier study [2] we considered the effect of elastic scattering of photoelectrons passing through a solid on the angular distribution of X-ray photoelectron intensity for a semi-infinite, flat, homogeneous sample. The angular distributions of photoelectrons were calculated by the Monte-Carlo method for some parameters of the elastic and inelastic interactions of electrons with a solid. It has been shown that taking account of elastic scattering can sometimes result in significant variation of both the angular

* For Part VI, see ref. 1

distribution and the absolute value of the photoelectron intensity compared to the values for photoemission from the free atoms or molecules, which are often used now in the interpretation of relative intensities in X-ray photoelectron spectra. Inelastic interaction was introduced by McGuire [3–5] in considering data on electron-impact ionization cross-sections of free atoms, while elastic interaction has been represented by the formula obtained using the first-order Born approximation within the scope of the Thomas–Fermi model [6, 7]

$$\sigma_{el} = (84.8/E)Z^{4/3} (\text{\AA}^2) \quad (1)$$

where $E(\text{eV})$ is the electron kinetic energy and Z is the atomic number of the scattering element

The following problems are considered in the present paper. Firstly, the estimations of the electron–atom elastic interaction cross-sections given in our previous paper [2] are improved, using the data of refs 8–11. Secondly, the results of Monte-Carlo calculations of the angular distributions of photoelectrons escaping from flat substrate samples covered with films of various thicknesses are presented. Neglect of elastic scattering is shown to lead to overestimated D/λ_n values (D being the film thickness, and λ_n the electron mean free path without inelastic collisions) derived either from the changes in photoelectron intensity with changes in D/λ_n or from the angular distribution of photoelectrons for fixed D/λ_n . Thirdly, the same calculation method is used to obtain the angular distributions of photoelectrons escaping from overlayer samples having various D/λ_n values. Once again, neglect of elastic scattering is shown to lead to overestimated D/λ_n values calculated conventionally on the basis of photoelectron angular distribution data using formulas derived without taking account of elastic scattering. The forms of the dependences obtained allow explanation of some discrepancies which arise on interpretation of the experimental data. Note that in the discussion given, the main conclusions can be understood without following the details of the calculation procedure.

CALCULATIONS

1 Elastic and inelastic interactions of electrons with a solid and the angular distribution of photoelectrons escaping from a flat, homogeneous sample

In ref 8 the total cross-sections for scattering of electrons by noble gases were evaluated over the energy range ~ 20 –2000 eV by the analysis of experimental and theoretical total cross-sections for elastic scattering, ionization and excitation. In ref 9 the total (elastic plus inelastic) cross-sections were measured for 0.1–500-eV electrons scattered by mercury atoms. Relying upon these data, it may be concluded that satisfactory agreement with experiment can be achieved for the inelastic interaction cross-section

σ_n by calculating the ionization cross-section according to refs 3–5 (this gives the major contribution to the inelastic interaction of atoms with electrons having kinetic energy in excess of 200 eV) For the elastic interaction cross-section σ_{el} good agreement is provided by calculations according to refs 10 and 11 We have compared (for various values of Z) the magnitudes of the elastic scattering cross-sections σ_{el} calculated using eqn (1) in the Thomas–Fermi approximation with those calculated using the expression

$$\sigma_{el} = 2\pi \int_0^\pi [f(\theta)]^2 \sin \theta d\theta \quad (2)$$

where the differential elastic scattering amplitude $f(\theta)$ was taken from refs 10 and 11 for $0^\circ < \theta < 158^\circ$, and assumed to be $f(158^\circ)$ for $\theta \geq 158^\circ$ The comparison reveals (see Table 1) that within the electron kinetic energy range of interest in X-ray photoelectron spectroscopy, eqn (1) gives total elastic scattering cross-sections σ_{el} of much greater magnitude than those calculated using eqn (2) with the data of refs 10 and 11 The difference increases with increasing atomic number Z and with decreasing kinetic energy of the electrons It is important to note that, together with the magnitude of the total elastic scattering cross-section, the anisotropy of the elastic scattering of photoelectrons on their passage through a solid [2] is of great significance in determining the extent of the elastic scattering effect on relative intensities in X-ray photoelectron spectra Within the same approximation used to derive eqn (1), the probability of elastic scattering of the electron by an atom at an angle θ can be written [2, 7] as

$$[f(\theta)]^2 = \sigma_{el} [A^2(1 + A^2)/(A^2 + \sin^2 \theta/2)^2] \quad (3)$$

where

$$A = 1.37(Z^{1/3}/E^{1/2}) \quad (4)$$

E (eV) being the electron kinetic energy, Z the atomic number of the scattering element, and A the parameter characterizing the extent of anisotropy of the elastic scattering of electrons We have calculated the mean scattering angle $\langle \theta \rangle$ on elastic collision for various values of Z and E using the following expression

$$\langle \theta \rangle = (2\pi/\sigma_{el}) \int_0^\pi \theta [f(\theta)]^2 \sin \theta d\theta \quad (5)$$

Using the data of refs 10 and 11 (see Table 1) and substituting eqn (3) into (5) we have

$$\langle \theta \rangle = \pi A^2 (\sqrt{1 + 1/A^2} - 1) \quad (6)$$

or

$$A = (\langle \theta \rangle) / (\pi \sqrt{1 - 2\langle \theta \rangle / \pi}) \quad (7)$$

Now, on the basis of eqn (7) it is possible to relate the differential cross-

TABLE 1

PARAMETERS OF ELASTIC AND INELASTIC INTERACTIONS OF ELECTRONS OF KINETIC ENERGY E WITH ATOMS

E (eV)	$\langle\theta\rangle^a$ ($^\circ$)	A^b	A^c	σ_{el}^d (\AA^2)	σ_{el}^e (\AA^2)	σ_n^f (\AA^2)	σ_{el}^d/σ_n
$Z = 6$							
100	49	0.40	0.25	2.60	9.25	2.24	1.16
250	31	0.21	0.16	1.50	3.70	1.19	1.26
500	22	0.14	0.11	0.92	1.85	0.69	1.33
1000	17	0.11	0.08	0.59	0.92	0.40	1.48
$Z = 18$							
100	56	0.51	0.36	4.23	40.0	3.41	1.24
250	42	0.32	0.23	2.75	16.0	2.51	1.1
500	29	0.20	0.16	1.96	8.0	1.62	1.21
1000	20	0.13	0.11	1.33	4.0	0.95	1.4
$Z = 54$							
100	60	0.58	0.52	4.17	173.0	9.33	0.45
250	37	0.27	0.33	4.85	69.2	5.44	0.9
500	28	0.19	0.23	3.84	34.6	3.28	1.17
1000	24	0.16	0.16	2.88	17.3	1.85	1.56
$Z = 80$							
100	35	0.25	0.59	8.71	292.3	7.1	1.23
250	30	0.20	0.37	5.74	116.9	4.2	1.37
500	40	0.30	0.26	3.7	58.5	2.3	1.61
1000	39	0.29	0.19	2.6	29.2	1.7	1.53

^a Mean scattering angle of electrons on elastic collision, calculated using eqn (5)^b Anisotropy parameter calculated for given $\langle\theta\rangle$ using eqn (7)^c Anisotropy parameter calculated using eqn (4)^d Total elastic scattering cross-section calculated using eqn (2) with the data of refs 10 and 11^e Total elastic scattering cross-section calculated using eqn (1)^f Electron-impact ionization cross-section taken for $Z = 6$ from refs 3–5 and for $Z = 18$, 54 and 80 from ref 8

sections for elastic scattering, calculated in refs 10 and 11, to the anisotropy parameter A . This allows us to use the calculation program of ref 2 and the results obtained there for the X , Y_0 , Y_1 , and Y_2 functions (these functions were introduced in ref 2 to allow determination of the angular distribution of photoelectrons escaping from a flat, homogeneous sample). The results of additional Monte-Carlo calculations are presented here for X , Y_0 , Y_1 , and Y_2 values obtained with the following parameters characterizing the electron–solid interaction: elastic to inelastic cross-section ratio $\sigma_{el}/\sigma_n = 1.0$ or 0.5 , and $A = 0.05$, 0.15 , 0.25 or 0.5 (see Table 2). A total of $\sim 10^5$ trajectories were calculated, with a maximum statistical error of 6% at a confidence limit of 0.682.

TABLE 2
 X , Y_0 , Y_1 AND Y_2 VALUES FOR SEMI-INFINITE SAMPLE, AS DEPENDENT ON THE ELECTRON ESCAPE ANGLE θ_{es} ,
 CALCULATED FOR VARIOUS MAGNITUDES OF A AND σ_{el}/σ_n

$\theta_{es} (^\circ)$	$A = 0.05$				$A = 0.15$				$A = 0.25$				$A = 0.5$			
	X	Y_0	Y_1	Y_2	X	Y_0	Y_1	Y_2	X	Y_0	Y_1	Y_2	X	Y_0	Y_1	Y_2
$\sigma_{el}/\sigma_n = 1$																
0-15	1.01	0.94	0.32	0.05	1.02	0.84	0.28	0.11	1.0	0.76	0.22	0.14	0.97	0.68	0.19	0.15
15-30	0.98	0.8	0.67	0.17	0.99	0.72	0.56	0.2	0.99	0.67	0.49	0.21	0.95	0.59	0.4	0.22
30-45	0.98	0.59	0.89	0.37	0.97	0.54	0.74	0.36	0.96	0.51	0.65	0.35	0.93	0.47	0.54	0.34
45-60	0.99	0.36	0.89	0.61	0.97	0.35	0.74	0.55	0.95	0.34	0.64	0.51	0.91	0.32	0.54	0.47
60-75	1.01	0.16	0.66	0.83	0.97	0.18	0.56	0.73	0.94	0.19	0.5	0.66	0.88	0.19	0.41	0.58
75-90	0.95	0.04	0.26	0.9	0.87	0.06	0.24	0.76	0.84	0.08	0.22	0.69	0.82	0.09	0.18	0.63
$\sigma_{el}/\sigma_n = 0.5$																
0-15	1.01	0.95	0.32	0.04	1.01	0.9	0.3	0.07	1.0	0.83	0.26	0.1	0.98	0.78	0.24	0.11
15-30	0.99	0.81	0.69	0.17	1.0	0.77	0.63	0.18	1.0	0.74	0.58	0.19	0.97	0.68	0.52	0.2
30-45	0.98	0.6	0.92	0.37	0.98	0.57	0.83	0.37	0.98	0.55	0.77	0.36	0.96	0.52	0.69	0.35
45-60	0.99	0.36	0.91	0.62	0.98	0.36	0.83	0.59	0.96	0.35	0.76	0.56	0.94	0.34	0.68	0.53
60-75	1.01	0.15	0.68	0.84	0.99	0.17	0.62	0.79	0.97	0.17	0.58	0.75	0.94	0.18	0.52	0.69
75-90	0.98	0.03	0.26	0.94	0.93	0.05	0.25	0.86	0.91	0.06	0.24	0.81	0.9	0.07	0.21	0.76

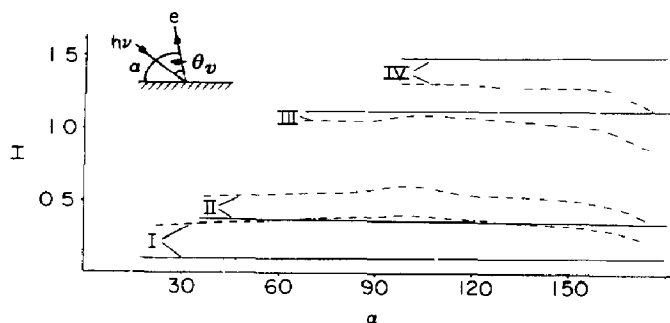


Fig 1 Angular distributions of photoelectron intensity I for a semi-infinite sample for $\beta = 2$ and various values of the angle θ_v between the direction of X-radiation and the direction of photoelectron escape $\theta_v = 15^\circ$ (I), 30° (II), 60° (III) and 90° (IV), (—) elastic scattering neglected, (----) both elastic and inelastic scattering considered, assuming $\sigma_{el}/\sigma_n = 1.0$ and $A = 0.25$

The effect of elastic scattering on the angular distribution of photoelectrons escaping from a flat, homogeneous sample was considered in detail in our previous paper [2]. It should be noted that the effects discussed there, relying on elastic scattering cross-section values obtained using eqn (1), now seem not so strong as was suggested, since more accurate calculations of σ_{el} [10, 11] and experimental data on the total (elastic plus inelastic) cross-sections for the electron-atom interaction [8, 9] have proved that eqn (1) is not fully consistent even for electron kinetic energies of ~ 1000 eV.

In Fig 1 the angular distributions of photoelectron intensity I for a flat, semi-infinite sample are shown, obtained by Monte-Carlo calculations assuming $\sigma_{el}/\sigma_n = 1$, $A = 0.25$, and a value of 2 for the photoionization anisotropy parameter β for the free atoms or molecules [12]. As can be seen from Fig 1, elastic scattering in this case results in a more isotropic photoelectron angular distribution compared to the initial distribution just after photoionization. The difference is greater for values of θ_v at the extremes of the $0-90^\circ$ interval, especially for the small values. The inclusion of elastic scattering can also be seen to decrease the value of I for values of the angle α (between the direction of photoelectron escape and the sample plane) greater than $\sim 160^\circ$. Note also that for the set of parameters concerned in Fig 1, the photoelectron angular distribution for $\theta_v \simeq 50-60^\circ$ hardly depends on whether or not elastic scattering is considered, these angles being close to the "magic" θ_v value for the angular distribution of photoelectrons on photoionization of the free atoms or molecules [12]. But in the general case, θ_v does depend on β , A and σ_{el}/σ_n .

2 Angular distributions of photoelectrons escaping from flat substrate samples covered with films of various thicknesses

As in ref 2, the Monte-Carlo method has here been used to calculate the angular distributions of photoelectrons escaping from flat substrates covered

with films having various values of D/λ_n . As obtained previously [2], the angular distribution of photoelectron intensity I for a flat, homogeneous sample is determined by the ratio σ_{el}/σ_n and by the differential elastic cross-section anisotropy parameter A . By analogy, the angular distribution of intensity I for the overlayer sample (see below), as well as that for the substrate covered with film, can be shown to depend on $(\sigma_{el}/\sigma_n)_{\text{film}}$, $(\sigma_{el}/\sigma_n)_{\text{substr}}$, A_{film} , A_{substr} and $D/\lambda_{n,\text{film}}$, where D is the film thickness and $\lambda_{n,\text{film}}$ the electron mean free path without inelastic collisions in the film. Moreover, the angular distribution of photoelectrons either from the overlayer or from the substrate covered with a film can be expressed using the X , Y_0 , Y_1 and Y_2 values determined in ref. 2 for the angular distribution of photoemission from a flat, homogeneous, semi-infinite sample, since the only condition there imposed on the system in order to derive these parameters was that of axial symmetry relative to the normal to the sample surface.

The angular distributions of photoelectrons escaping from flat, homogeneous substrates covered with films of various thicknesses were calculated by the Monte-Carlo method assuming the following parameters characterizing the electron-solid interaction: the elastic to inelastic cross-section ratio was taken to be unity for both the film and the sample, and values of A of 0.25 and 0.1 were adopted for film and substrate respectively. A total of 10^5 trajectories were calculated, the corresponding statistical error being $\sim 2\%$ for a confidence limit of 0.682. The X , Y_0 , Y_1 and Y_2 values obtained for various D/λ_n are presented in Table 3. It should be remembered that in the computation scheme employed [2], the angular distribution of photoelectrons was evaluated by comparing the numbers of escaped electrons having trajectories within each one of six intervals of the escape angle θ_{es} measured from the normal to the surface: $0-15^\circ$, $15-30^\circ$, $30-45^\circ$, $45-60^\circ$, $60-75^\circ$, and $75-90^\circ$. To account for the finite θ_{es} intervals used in the calculations, the average escape-angle for each interval was not taken simply to be 7.5° , 22.5° , etc., but was calculated using the equation

$$\int_{\theta_m}^{\theta_{m+1}} \exp(-D/\lambda_n \cos \theta) \sin \theta d\theta \bigg/ \int_{\theta_m}^{\theta_{m+1}} \sin \theta d\theta = \exp[-D/(\lambda_n \cos \theta_m^*)] \quad (8)$$

where $\theta_m = 15^\circ(m-1)$, $m = 1, 2, \dots, 6$. The results for θ_m^* obtained for some D/λ_n values are shown in Table 4. Equation (8) accounts for the non-uniformity of the distribution of photoelectrons within each θ_{es} interval ($0-15^\circ$, $15-30^\circ$, etc.) used in the calculations.

In Fig. 2 the angular distributions of photoelectron intensity I for substrates covered with films of various thicknesses are shown, calculated on the basis of the data of Table 3 using expression (34) from ref. 2. Two well-defined effects observed in Fig. 2 should be noted to be related to the elastic scattering. The first is the sharper decay of the substrate photoelectron intensity with increasing D/λ_n as compared to the case where elastic scattering of electrons in the solid is neglected. Let us denote by DL the D/λ_n ratio

TABLE 3

X, Y_0 , Y_1 AND Y_2 VALUES CHARACTERIZING PHOTOELECTRON INTENSITY FOR SUBSTRATE SAMPLE COVERED WITH FILMS OF VARIOUS THICKNESSES

$\theta_{es} (^\circ)$	$D/\lambda_n = 0$				$D/\lambda_n = 0.2$				$D/\lambda_n = 0.6$			
	X	Y_0	Y_1	Y_2	X	Y_0	Y_1	Y_2	X	Y_0	Y_1	Y_2
0-15	1.01	0.76	0.27	0.14	0.79	0.58	0.2	0.12	0.48	0.33	0.1	0.07
15-30	0.98	0.66	0.48	0.22	0.77	0.5	0.35	0.17	0.46	0.29	0.18	0.1
30-45	0.95	0.5	0.64	0.35	0.72	0.37	0.44	0.25	0.39	0.2	0.21	0.13
45-60	0.95	0.34	0.62	0.52	0.65	0.24	0.39	0.33	0.3	0.12	0.15	0.13
60-75	0.94	0.19	0.51	0.66	0.49	0.12	0.25	0.3	0.16	0.06	0.07	0.07
75-90	0.8	0.08	0.16	0.65	0.2	0.05	0.08	0.11	0.06	0.02	0.02	0.02

$\theta_{es} (^\circ)$	$D/\lambda_n = 1.0$				$D/\lambda_n = 2.0$			
	X	Y_0	$10Y_1$	$10Y_2$	$10X$	$10Y_0$	$100Y_1$	$100Y_2$
0-15	0.29	0.19	0.52	0.44	0.76	0.47	0.97	1.17
15-30	0.27	0.16	0.9	0.56	0.65	0.38	1.53	1.23
30-45	0.21	0.11	0.94	0.61	0.45	0.24	1.13	1.04
45-60	0.14	0.06	0.61	0.49	0.25	0.13	0.68	0.6
60-75	0.07	0.03	0.24	0.23	0.12	0.06	0.23	0.25
75-90	0.03	0.01	0.08	0.07	0.05	0.02	0.09	0.1

TABLE 4
 θ_m^* VALUES CALCULATED USING EQN (8)

D/λ_n	$\theta_{es} (m)$					
	0–15° (1)	15–30° (2)	30–45° (3)	45–60° (4)	60–75° (5)	75–90° (6)
0.2	10.37	23.46	38.21	53.14	68.17	82.39
0.6	10.36	23.44	38.17	53.05	67.51	80.39
1.0	10.36	23.43	38.13	52.56	67.26	79.41
2.0	10.35	23.38	38.04	52.35	66.32	78.26

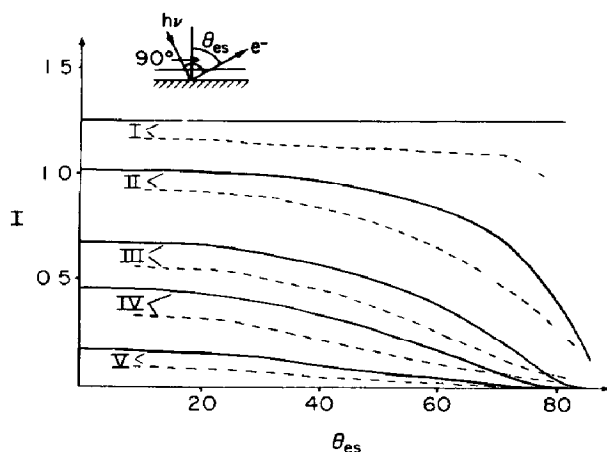


Fig. 2 Angular distributions of photoelectron intensity I for substrates covered with films of various thicknesses $D/\lambda_n = 0$ (I), 0.2 (II), 0.6 (III), 1.0 (IV) and 2.0 (V), $\beta = 1$, (—) elastic scattering neglected, (----) both elastic and inelastic scattering considered

expressed by the usual formulas derived without taking account of elastic scattering of photoelectrons (see eqn (9)). In Table 5 are shown, as a function of D/λ_n and θ_{es} , the DL values calculated using the expression

$$I(D/\lambda_n) = I_0 \exp(-DL/\cos \theta_m^*) \quad (9)$$

where I_0 and $I(D/\lambda_n)$ are the photoelectron intensities for the clean and the film-covered samples respectively, obtained by the Monte-Carlo method and taking into account both elastic and inelastic interactions of the electrons with the solid. Substitution of the calculated I_0 and $I(D/\lambda_n)$ values into eqn (9) allows simulation of the dependence of the experimental data on elastic scattering. It follows from Table 5 that $DL > D/\lambda_n$ for $\theta_{es} < 60^\circ$, owing probably to the fact that elastic scattering leads to an increase in the distance between the point of photoionization and that of electron escape from the solid, which is equivalent formally to an increase in D or a decrease in λ_n .

TABLE 5
DL VALUES CALCULATED USING EQN (9)

D/λ_n	$\theta_{es} (^\circ)$					
	0-15	15-30	30-45	45-60	60-75	75-90
0.2	0.241	0.224	0.23	0.24	0.26	0.203
0.6	0.737	0.712	0.724	0.733	0.718	0.484
1.0	1.24	1.214	1.23	1.22	1.087	0.504
2.0	2.574	2.535	2.48	2.32	1.88	1.143

The second feature to be noted in Fig 2 is that for $\theta_{es} > 60^\circ$, a decrease in the DL value compared to D/λ_n takes place. With $D/\lambda_n = 0.6$ and $\theta_{es} \geq 80^\circ$ the photoelectron intensity calculated by the Monte-Carlo method exceeds even the value obtained without taking account of elastic scattering. A possible explanation of such behaviour is that, for sufficiently thick films and large θ_{es} values, the significant contribution to photoelectron intensity is that from electrons ejected in a direction close to the surface normal immediately after the photoionization event and scattered by a large angle near the outer surface of the film covering the sample. Such an explanation seems to be quite reasonable considering that the average scattering-angle on collision of an electron with an atom is sufficiently large for $A = 0.25$ (see Table 1).

We have used the least-squares method to analyze the photoelectron angular distribution shown in Fig 2 for a film-covered sample. The condition

$$\sum_{m=1}^k [I_m - C \exp(-DL/\cos \theta_m^*)]^2 = \min \quad (10)$$

was used to obtain C and DL values for various $k = 2, 3, \dots, 6$, with θ_m^* being determined by eqn (8) (see also Table 4) and I_m being the average intensity of photoelectrons escaping within the interval $15^\circ(m-1) < \theta_{es} < 15^\circ(m)$, as calculated by the Monte-Carlo method with the photoionization anisotropy parameter $\beta = 1$. The results are shown in Table 6. Taking various integral values of k it is possible to follow qualitatively the changes in the DL and C values with the value of θ_{es} used in the calculation of the angular distribution. It should be noted that with neglect of elastic scattering (see ref. 2 for details), we have

$$I_m = [1 + \beta/2(3/2 \cos^2 \theta_v - 1)] \exp[-D/(\lambda_n \cos \theta_m^*)] \quad (11)$$

and hence, with $\beta = 1$ and $\theta_v = 90^\circ$ (see Fig 2),

$$\left. \begin{aligned} C &= 1.25 \\ DL &= D/\lambda_n \end{aligned} \right\} \quad (12)$$

TABLE 6

RESULTS OF LEAST-SQUARES ANALYSIS^a OF PHOTOELECTRON ANGULAR DISTRIBUTIONS^b FOR SUBSTRATE SAMPLE COVERED WITH FILMS OF VARIOUS THICKNESSES

k	$D/\lambda_n = 0.2$		$D/\lambda_n = 0.6$		$D/\lambda_n = 1.0$		$D/\lambda_n = 2.0$	
	DL	C	DL	C	DL	C	DL	C
2	0.33	1.29	0.7	1.13	1.15	1.07	2.24	0.84
3	0.38	1.35	0.85	1.38	1.35	1.32	2.23	0.83
4	0.32	1.26	0.79	1.24	1.24	1.17	2.02	0.664
5	0.29	1.22	0.71	1.13	1.12	1.03	1.88	0.57
6	0.24	1.14	0.71	1.12	1.11	1.01	1.88	0.57

^a See eqn (10) in text

^b Calculated by Monte-Carlo method

The above-mentioned effects of the elastic scattering in a solid on the angular distribution of escaping photoelectrons are clearly apparent from Table 6. For the first, the DL values do almost always exceed the ratio D/λ_n , and likewise $C < 1.25$. For the second, the DL value decreases with increasing k , behaviour equivalent to the account given by eqn (10) for the contribution from photoelectrons escaping at large θ_{es} .

3 Angular distribution of photoelectrons escaping from a flat, homogeneous overlayer

The Monte-Carlo calculation of the angular distribution of photoelectrons escaping from a flat overlayer, and the least-squares analysis of the results, did not differ significantly from the procedures described in the preceding section of this paper. A total of 1.5×10^6 trajectories were calculated, with a resulting statistical error of 1% for the 0.682 confidence limit. The X , Y_0 , Y_1 and Y_2 values obtained are presented in Table 7. The following condition was used instead of eqn (10)

$$\sum_{m=1}^k \{I_m - C[1 - \exp(-DL/\cos \theta_m^*)]\}^2 = \min \quad (13)$$

where $k = 3, 4, 5, 6$ and I_m is the average intensity of photoelectrons escaping from the overlayer within the interval $15^\circ(m-1) < \theta_{es} < 15^\circ(m)$, calculated by the Monte-Carlo method with the photoionization anisotropy parameter $\beta = 1$ (see Fig. 3). The DL and C values obtained using eqn (13) are shown in Table 8. As in Section 2 above, the equalities given in eqn (12) should hold for the case where elastic scattering is neglected. As can be seen from the data of Fig. 3 and Table 8, only one of the two effects of elastic scattering on angular distribution as noted in the preceding section is exhibited in the case under consideration, this being the increase in the

TABLE 7

X , Y_0 , Y_1 AND Y_2 VALUES CHARACTERIZING PHOTOELECTRON INTENSITY FOR OVERLAYER SAMPLES OF VARIOUS THICKNESSES

$\theta_{es} (^{\circ})$	$D/\lambda_n = 0.2$				$D/\lambda_n = 0.6$			
	X	Y_0	Y_1	Y_2	X	Y_0	Y_1	Y_2
0-15	0.19	0.17	0.06	0.02	0.5	0.42	0.15	0.08
15-30	0.21	0.16	0.14	0.05	0.52	0.38	0.31	0.14
30-45	0.24	0.14	0.21	0.1	0.57	0.31	0.45	0.26
45-60	0.3	0.1	0.25	0.2	0.65	0.22	0.49	0.43
60-75	0.43	0.06	0.25	0.37	0.76	0.13	0.43	0.63
75-90	0.63	0.03	0.15	0.6	0.75	0.05	0.19	0.69

$\theta_{es} (^{\circ})$	$D/\lambda_n = 1.0$				$D/\lambda_n = 2.0$			
	X	Y_0	Y_1	Y_2	X	Y_0	Y_1	Y_2
0-15	0.68	0.56	0.18	0.13	0.9	0.7	0.22	0.19
15-30	0.71	0.51	0.4	0.21	0.92	0.63	0.47	0.29
30-45	0.76	0.41	0.56	0.35	0.93	0.5	0.64	0.43
45-60	0.81	0.28	0.59	0.53	0.93	0.33	0.64	0.6
60-75	0.86	0.16	0.47	0.7	0.92	0.18	0.49	0.74
75-90	0.78	0.06	0.21	0.72	0.81	0.07	0.21	0.74

TABLE 8

RESULTS OF LEAST-SQUARES ANALYSIS^a OF PHOTOELECTRON ANGULAR DISTRIBUTIONS^b FOR OVERLAYER SAMPLES OF VARIOUS THICKNESSES

k	$D/\lambda_n = 0.2$		$D/\lambda_n = 0.6$		$D/\lambda_n = 1.0$		$D/\lambda_n = 2.0$	
	DL	C	DL	C	DL	C	DL	C
3	—	—	0.72	0.11	0.99	1.22	1.98	1.15
4	0.14	1.75	0.76	1.07	1.25	1.09	2.38	1.09
5	0.21	1.22	0.8	1.04	1.31	1.06	2.52	1.09
6	0.34	0.83	0.99	0.94	1.6	0.98	3.46	1.04

^a See eqn (13) in text

^b Calculated by Monte-Carlo method

effective distance covered by the photoelectron between the photoionization and escape events. This suggestion is confirmed by $DL > D/\lambda_n$, this inequality becoming greater on increase in D/λ_n . The magnitude of C is only slightly dependent on D/λ_n . The increase in DL with θ_{es} above 60° is due to the decrease in the photoelectron intensity at such angles (see Fig. 3). It should be noted that this is similar to the case for a semi-infinite, flat, homogeneous

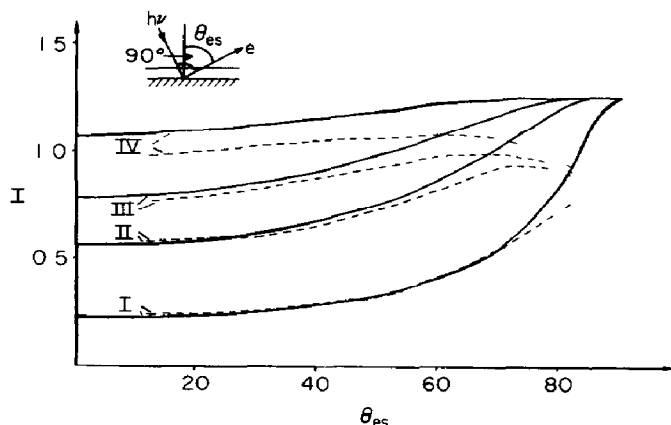


Fig 3 Angular distributions of photoelectron intensity I for overlayer samples of various thicknesses $D/\lambda_n = 0.2$ (I), 0.6 (II), 1.0 (III) and 2.0 (IV), $\beta = 1$, (—) elastic scattering neglected, (---) both elastic and inelastic scattering considered

sample, as considered in ref 2 and in Section 1 above. In both cases the major contribution to the intensity is suggested to be that from the photoelectrons generated in the uppermost layers of the sample and undergoing a small number of elastic collisions before escape from the solid.

DISCUSSION OF RESULTS

(a) Flat, semi-infinite sample

The calculation reveals the elastic scattering to produce an "isotropization" in the angular distribution of photoelectrons that is formally equivalent to a decrease in $|\beta|$. Due to this effect the experimental photoelectron intensity for a small angle θ_v between the direction of X-radiation and that of photoelectron escape should exceed the theoretical values obtained with elastic scattering neglected (Fig 1). For large θ_v (up to 90°) the latter theoretical values should exceed the experimental ones. Some decrease in photoelectron intensity must be observed for a large angle α between the sample plane and the escape direction (Fig 1). All these facts allow of experimental verification, but no relevant experimental data are available in the literature. One complication involved in experimental verification of the last effect, concerning the decrease in intensity for large α , is that a similar decrease can be caused by the presence of a thin surface-contamination layer, as well as by the analyzer entrance-slit projection onto the sample plane exceeding the sample area irradiated.

(b) Film-covered sample

According to the calculations, the substrate-peak intensity will here be decreased due to elastic scattering, the relative effect being greater as the

film thickness D increases. The opposite behaviour should be observed for large escape-angles, because of the significant contribution to intensity from photoelectrons covering the distance to the surface at a small angle to the normal (much smaller than θ_{es}) and then being scattered elastically near the surface to escape at θ_{es} .

The intensity I of the substrate photoelectron-peak is often used to calculate the D/λ_n ratio, where λ_n is the photoelectron mean free path without inelastic collisions in the film. If this calculation is performed for fixed $\theta_{es} < 60^\circ$ using eqn (9), which does not take account of elastic scattering, then the DL value formally obtained will exceed the real D/λ_n ratio. With the set of parameters adopted in our calculations the difference would usually be $\sim 20\%$. For $\theta_{es} > 60^\circ$ the inequality may be reversed (see Table 5). It should be emphasized that the photoelectron intensities I calculated taking account of elastic scattering, and, hence, the experimental I values, can be represented with sufficient accuracy by eqn (9), but in general the DL values so obtained will not coincide with the real D/λ_n values. Therefore, underestimated $\lambda_{n(\text{form})}$ values are usually obtained from eqn (9), since it can be shown that

$$\lambda_{n(\text{form})}^{-1} = \lambda_n^{-1} + a\lambda_{e1}^{-1} \quad (14)$$

where a is a coefficient to account for the elastic-scattering contribution, and λ_{e1} is the electron mean free path without elastic collisions. It should be noted that values of $\lambda_{n(\text{form})}$ have also been determined [13] using the expression for the photoelectron intensity for a flat, homogeneous sample

$$I = K_0 \lambda_{n(\text{form})} n \sigma P_{\text{free}} \quad (15)$$

where K_0 is the instrument factor, σ the photoionization cross-section, n the density, and P_{free} the photoionization angular distribution for the free atoms or molecules. But this should in fact (see ref. 2 and the present paper) be

$$I = K_0 \lambda_n n \sigma P_{\text{solid}} \quad (16)$$

where P_{solid} is the photoionization angular distribution for a solid. By virtue of eqns (15) and (16),

$$P_{\text{free}} \lambda_{n(\text{form})} = P_{\text{solid}} \lambda_n \quad (17)$$

where $P_{\text{free}}/P_{\text{solid}} > 1$ for $\theta_v = 90^\circ$ (see Figs 1 and 2). Hence, eqn (15), when formally used, also gives increased $\lambda_{n(\text{form})}$ values, although the increase is usually less pronounced ($P_{\text{free}}/P_{\text{solid}} = 0.9$ with the parameters used in our calculations).

Equation (9) is also used to obtain the λ_n value for the case of fixed film-thickness D and variable angle θ_{es} (see for example refs 14 and 15). In ref. 14 the value of λ_n was observed to increase with θ_{es} (for $D/\lambda_n \simeq 2.2$, and $35^\circ < \theta_{es} < 80^\circ$) and the effect was supposed due either to overlayer patching or to sample-surface roughness (or to both). The λ_n values calcu-

TABLE 9

λ_n VALUES AS DEPENDENT ON THE PHOTOELECTRON ESCAPE ANGLE θ_{es} , CALCULATED USING THE EXPERIMENTAL DATA^a

θ_{es} (°)	λ_n^b (nm)	λ_n^c (nm)
80	12.0	0-8.0
70	7.5	4.0
60	5.6	4.0
52	4.9	4.1
40	4.3	3.6
35	4.2	3.6

^a From ref. 14

^b Calculated using eqn (9) with the experimental data from ref. 14

^c Values corrected to account for possible overlayer-patching

lated for the various values of θ_{es} used in ref. 14 are shown in Table 9. It will be noted that even the patch-corrected λ_n values still slightly increase with increasing θ_{es} . We suppose this dependence of λ_n on θ_{es} to be explained by the elastic scattering of photoelectrons in a solid. Indeed, as can be seen from Table 5, for $D/\lambda_n = 2.0$, the inclusion of elastic scattering results in a decrease in the value of DL calculated using eqn (9), with increasing θ_{es} , which is equivalent to an increase (with θ_{es}) in the value of λ_n obtained using the same formula. Therefore, the dependence of λ_n (as calculated using eqn (9)) on θ_{es} , observed in ref. 14, can be attributed not only to the presence of sample-surface defects, but also to the effect of elastic scattering of electrons in a solid on the photoelectron intensity.

(c) Overlayer sample of finite thickness

The calculation shows that the peak intensity of photoelectrons escaping from an overlayer of finite thickness can be written in the form of an expression derived with no account of elastic scattering (see Fig. 3).

$$I = C[1 - \exp(-DL/\cos \theta_m^*)] \quad (18)$$

The values of C and DL obtained from eqn (18) are different from the real C and D/λ_n values. For example (see Table 8), C values within the interval 0.8-1.75 are obtained for $\beta = 1$ and $\theta_v = 90^\circ$, instead of $C = 1.25$. The DL values not only differ noticeably from the real D/λ_n values, but depend on the set of escape-angle (θ_{es}) values used in the calculations (see Table 8, where the θ_{es} interval is determined, by the condition that k is integral, to be $0 < \theta_{es} < 15^\circ(k)$). The change in DL value as a function of k was analyzed in ref. 15 on the basis of experimental data taken from the literature,

and DL was found to increase with k . This is confirmed by the data of Table 8. Therefore, elastic scattering, together with surface roughness, can produce an increase in DL with increasing θ_{es} interval.

(d) *Film/substrate intensity ratio*

The above results can be readily applied to the D/λ_n values determined on the basis of the film/substrate intensity ratio

$$I_{\text{film}}/I_{\text{substr}} = R\{1 - \exp[-D/(\lambda_n \cos \theta_{es})]\} \exp[D/(\lambda_n \cos \theta_{es})] \quad (19)$$

where R is the ratio of the intensities for a film of infinite thickness and for the clean substrate. In ref. 16 experimental angular distributions of photoelectron intensity were reported for silicon samples covered with oxide layers of various thicknesses. Figure 4(a) shows the dependence of $\ln[I_{\text{film}}/(I_{\text{substr}}R) + 1]$ on $1/\cos \theta_{es}$ for $R = 0.672$ (data taken from refs. 15 and 16). The deviation from the linear law was again [16] explained as being due to sample-surface imperfection. In Fig. 4(b) the dependence of $\ln(I_{\text{film}}/I_{\text{substr}} + 1)$ on $1/\cos \theta_{es}$ is presented for I_{film} and I_{substr} calculated by the Monte-Carlo method (see Figs. 2 and 3 and Tables 3 and 6). The evident qualitative correlation between the two figures suggests that the nonlinear dependence of $\ln(I_{\text{film}}/I_{\text{substr}} + 1)$ on $1/\cos \theta_{es}$ can be explained also by the effect of elastic scattering of electrons. The possibility that elastic scattering might explain the results shown in Fig. 4(a) was also considered in ref. 16, but the complications involved in the evaluation of the extent of this effect

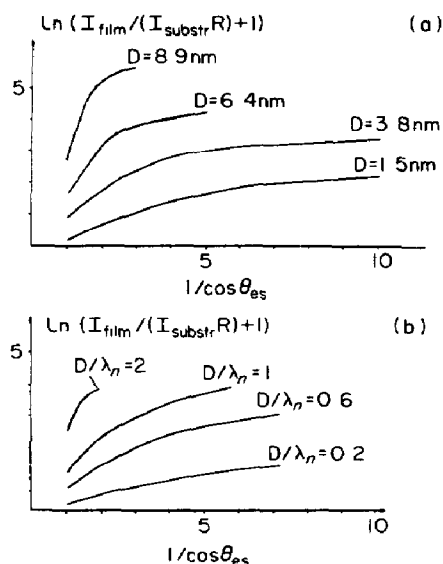


Fig. 4. Dependence of $\ln[I_{\text{film}}/(I_{\text{substr}}R) + 1]$ on $1/\cos \theta_{es}$ (a) as taken from refs. 15 and 16, $R = 0.672$, and (b) drawn using the I_{film} and I_{substr} values calculated in the present paper, $R = 1$.

led the authors to conclude that sample-surface roughness played the major role

Therefore, it can be concluded that the elastic-scattering effect often explains, without any additional assumptions, the experimentally observed discrepancies produced by the application of formulas derived without taking account of elastic scattering. It is quite evident, of course, that the influence of other factors such as surface roughness, overlayer patching, etc., can also lead to discrepancies between experiment and the theory that does not take account of elastic scattering [15]

REFERENCES

- 1 V G Yarzhevsky and V I Nefedov, *J Electron Spectrosc Relat Phenom*, 19 (1980) 123
- 2 O A Baschenko and V I Nefedov, *J Electron Spectrosc Relat Phenom*, 17 (1979) 405
- 3 E J McGuire, *Phys Rev A*, 3 (1971) 267
- 4 E J McGuire, *Phys Rev A*, 16 (1977) 62
- 5 E J McGuire, *Phys Rev A*, 20 (1979) 452
- 6 B L Henke, *J Phys (Paris)*, C4, 32 (1971) 115
- 7 N F Mott and H S W Massey, *The Theory of Atomic Collisions*, Clarendon Press, Oxford, 1965
- 8 F J de Heer, R U J Jansen and W van der Kaay, *J Phys B*, 12 (1979) 979
- 9 K Jost and B Ohnemus, *Phys Rev A*, 19 (1979) 641
- 10 M Fink and A C Yates, *At Data*, 1 (1970) 385
- 11 M Fink and J Ingram, *At Data*, 4 (1972) 129
- 12 J Cooper and R Zare, *J Chem Phys*, 48 (1968) 942
- 13 S Evans, R G Pritchard and J M Thomas, *J Phys C*, 10 (1977) 2483
- 14 C R Brundle, H Hopster and J D Swallen, *J Chem Phys*, 70 (1979) 5190
- 15 M F Ebel, *J Electron Spectrosc Relat Phenom*, 141 (1978) 287
- 16 J M Hill, D G Royce, C S Fadley, L F Wagner and F J Grunthaner, *Chem Phys Lett*, 44 (1976) 225